Available online at www.sciencedirect.com
ScienceDirect
Mechatronics 17 (2007) 489–500
MECHATRONICS

Advanced mechatronic design using a multi-objective genetic algorithm optimization of a motor-driven four-bar system

Zouhaier Affi [a], Badreddine EL-Kribi [a], Lotfi Romdhane [b,*]

[a] Laboratoire de Génie Mécanique, Ecole Nationale d'Ingénieurs de Monastir, Monastir 5019, Tunisia
[b] Laboratoire de Génie Mécanique, Ecole Nationale d'Ingénieurs de Sousse, Sousse 4000, Tunisia

Received 2 June 2006; accepted 5 June 2007

Abstract

In this work we present a genetic algorithm based method to design a mechatronic system. First, we present the sequential approach where we optimize the geometry of the mechanism, for a given path, and then solve the dynamic problem where we take into account the characteristics of the motor along with the inertia of the different links of the mechanism. Several types of objective functions are tested. We show, however, that this sequential method does not yield acceptable results for the dynamic behavior due to the fact that the geometry is assumed fixed when optimizing the dynamics. This led us to formulate a global optimization problem where all the parameters of the mechanism are considered simultaneously. The problem is then presented as a multi-objective optimization one where the geometry and the dynamics are considered simultaneously. The obtained solutions form what is called a "Pareto front" and they are analyzed for several different design conditions. This paper also shows the advantages of a multi-objective optimization approach over the single-objective one.

Keywords: Advanced mechatronic design; Genetic algorithms; Mechanism synthesis; Multi-objective optimization

1. Introduction

The traditional approach, for robot design process, is usually made of two sequential phases: the mechanical design, during which the geometry of the mechanism is determined, followed by the control system design, where the problem of the dynamic behavior is considered. The mechanical structure of a mechanism is usually determined in advance without considering the corresponding control system. This approach yields an electromechanical system, with high mechanical performance, in which the dynamic behavior is not usually acceptable. Control action may be hindered by hardware limitations even if much effort has been made on the sophisticated advanced controller [3,9].

The research trend in modern mechanical systems development is the mechatronic approach. The key idea of the mechatronic methodology is to create an integrated design environment that enables strictly simultaneous designs for mechanical structures, the control strategy and even the interaction of the whole system with its environment. The goal of this philosophy is to achieve an optimal mechatronic system performance.

Recently, the mechatronic system design attracted several researches [1,4,6]. An integrated design and PD control of high-speed four-bar mechanism is presented in [1]. In this work, the authors showed that the result of the controller can be significantly improved by using the Design For Control (DFC) strategy. The key idea of this approach is to find the best mass distribution in the mechanism to facilitate the control strategy. In order to facilitate a controller design and improve tracking performance for high-speed system, the mechatronic approach suggests a

* Corresponding author.
E-mail addresses: zouhaier.affi@enim.rnu.tn (Z. Affi), kribi_badreddine@yahoo.fr (B. EL-Kribi), lotfi.romdhane@enim.rnu.tn (L. Romdhane).

0957-4158/$ - see front matter © 2007 Elsevier Ltd. All rights reserved.
doi:10.1016/j.mechatronics.2007.06.003

negative masse-redistribution scheme that simplifies the dynamic model [4].

Another idea in the design of mechatronic systems is based on the hybrid machine concept [2,11]. These machines are made of a mechanism driven simultaneously by a servomotor and a constant velocity (CV) motor [2]. The integration of CV motor can reduce significantly the peak torque and the power in the servomotor which acts as a low torque modulator. However, this method requires a complicated control strategy for the mechatronic system. In [11] a hybrid cam mechanism was used to combine the classical single motor solution and the servo solution. The servo motor superimposes its motion on the CV of the main motor. As a result, the hybrid cam mechanism adds more flexibility to the system requiring only small peak power and peak torque from the servo motor.

Other researchers used the genetic algorithm (GA) and the fuzzy logic to synthesize mechanisms and control strategies for electromechanical systems [7,8,10,12]. The GA optimization method was also used in [15] for the concurrent optimal design of a modular robotic configuration. Based on the multi-objective optimization the authors seek to find simultaneously the type and the dimensions of robotic systems.

In this paper, we present the synthesis of mechatronic systems based on the GA evolutionary technique. The first goal of this work is to find the optimal dimensions of the links to minimize the error between the actual coupler curve and the desired path. Then, this mechanism is optimized to have the best dynamic behavior, i.e., a minimum torque in the motor and a minimum torque fluctuation. Since the torque, generated by the motor is proportional to the current, and in order to introduce the motor parameter in the optimization process, we will be interested, in this work, in optimizing the current rather than the torque. Several objective functions are tested: the maximum current, the current variation and the current fluctuation in the motor. However, we show that optimizing one objective function at one time cannot lead to satisfactory designs. Indeed, once the geometry is fixed by the path synthesis problem, it becomes difficult to get satisfactory dynamic behavior for the given link lengths. Moreover, optimizing the maximum current for example can lead to high current fluctuations and vice versa. Therefore, we present an alternative formulation based on the multi-objective function optimization, where the designer can specify several objective functions simultaneously and all optimal results are presented as a hyperplane called "Pareto front". The main advantages of this method are its simplicity of implementation and its fast convergence to optimal solutions with no deep knowledge of the search domain. Moreover, the designer obtains several possible solutions and he can choose the one that suites best his application.

This paper is organized as follows: in Section 2, we present the problem formulation in the general case. Section 3 describes the dimensional synthesis of the four-bar mechanism for a specified path. The mathematical model of the motor-driven mechanism system is presented in Section 4. In Section 5, the results of the different optimization problems are presented along with the multi-objective optimization, which takes into account all the objective functions simultaneously. Some concluding remarks are given in Section 6.

2. Formulation of the problem

In this paper, we will consider the following problems:

For a desired path of a tracing point on the coupler of a four-bar mechanism, find the optimal dimensions of the mechanism. For this optimized mechanism, find the set of mechanisms that minimize one of the following objective functions: the maximum current, the current variation, and the current fluctuation. Finally, the global problem is considered, which aims to find the mechanism that can optimize all the above mentioned objective functions simultaneously.

The optimization problems can be formulated as follows:

$$\text{min:} \quad f_j(X), \quad j = 1, \ldots, m \tag{1}$$

$$\text{subject to:} \quad g_k(X) \leqslant 0, \quad k = 1, \ldots, n$$
$$x_i \in [x_{i\min}, x_{i\max}]; \quad x_i \in X \tag{2}$$

f_j is the objective function,
g_k is the constraint applied to the system,
X is a design vector of the mechatronic system, which contains all the independent design variables,
$x_{i\min}$ and $x_{i\max}$ define the limits of each design variable x_i.

The multi-objective optimization can be replaced by a mono-objective one using weighting factors as follows:

$$f = \sum_{j=1}^{m} \alpha_j f_j(X) \tag{3}$$

where α_j's are arbitrary factors, f_j $(j = 1, \ldots, m)$ are the objective functions to be optimized.

The choice of weighting factors α_i is arbitrarily made by the user and it is not usually justified. Changing these weighting factors changes the optimal solution. To avoid this problem and to obtain all possible solutions, the multi-objective function is used. The idea behind this method is to find all possible solutions optimizing simultaneously all the objective functions.

The GA method will be used to solve these problems.

3. Dimensional synthesis model

Fig. 1 shows a general four-bar mechanism. In general, an effective torsional spring with a constant stiffness k and an effective torsional damper with damping coefficient c are attached to the follower of the four-bar mechanism.

The spring and the damper represent an external load applied to the mechanism.

The objective function is calculated as the sum of the errors between each desired point and the obtained one. Let C_d^i be a desired location of the tracing point

$$C_d^i = [C_{xd}^i, C_{yd}^i]^{\mathrm{T}} \tag{4}$$

And let C_r^i be the obtained location of the tracing point

$$C_r^i = [C_{xr}^i(\Phi_2^i), C_{yr}^i(\Phi_2^i)]^{\mathrm{T}} \tag{5}$$

$$\begin{cases} C_{xr} = x_0 + L_2\cos\Phi_2 + r_{cx}\cos\Phi_3 - r_{cy}\sin\Phi_3 \\ C_{yr} = y_0 + L_2\sin\Phi_2 + r_{cx}\sin\Phi_3 + r_{cy}\cos\Phi_3 \end{cases} \tag{6}$$

All the parameters are defined in Fig. 1.
Where the constraints to be satisfied are

- Counter clockwise rotation of the crank

$$g_1(X) : \Phi_{2,i+1} - \Phi_{2,i} > 0 \quad (i = 1, \ldots, N) \tag{7}$$

N is the number of points used to descretize the desired path.

- The Grashoff condition

$$g_2(X) : L_1 + L_2 < L_3 + L_4; \quad L_2 < L_3 < L_4 < L_1 \tag{8}$$

- Each design variable is confined within a given range

$$g_3(X) : x_i \in [x_{i\min}, x_{i\max}], \quad x_i \in X \tag{9}$$

The design vector is given by

$$X = [x_0, y_0, \theta_0, L_i, \Phi_{2j}, r_{cx}, r_{cy}]^{\mathrm{T}} \tag{10}$$

where

θ_0 is the orientation angle of link 1,
Φ_{2j} $(j = 1, \ldots, N)$ is the crank angle corresponding to the jth point to generate on the path,
r_{cx} and r_{cy} are the local coordinates of the coupler point.

The objective function to be minimized is given by

$$f_1 : \min \left(\left(\sum_{i=1}^{N} [(C_{xd}^i - C_{xr}^i)^2 + (C_{yd}^i - C_{yr}^i)^2] \right)^{\frac{1}{2}} + M_1 h_1(X) + M_2 h_2(X) + M_3 h_3(X) \right) \tag{11}$$

$h_i(X)$ $(i = 1, 2, 3)$ is equal to zero if the constraint $g_i(X)$ is satisfied and equal to one otherwise. M_i is a high value number that penalizes the objective function when the associated constraint is not satisfied [8,10].

4. Mechatronic system model

In this section, the motor-mechanism system is treated as a single mechatronic system. In traditional design methodology, when a motor is coupled to a mechanism, a periodically time varying torque is produced due to the changing inertia of the mechanism during the motion. This torque variation is undesirable when timing requirements are involved, which requires the design of a complex controller. The torque fluctuation produces undesirable loading of the motor. Moreover, the maximum torque needs much more power for the same task [2]. In this advanced mechatronic design, we will use the GA technique in order

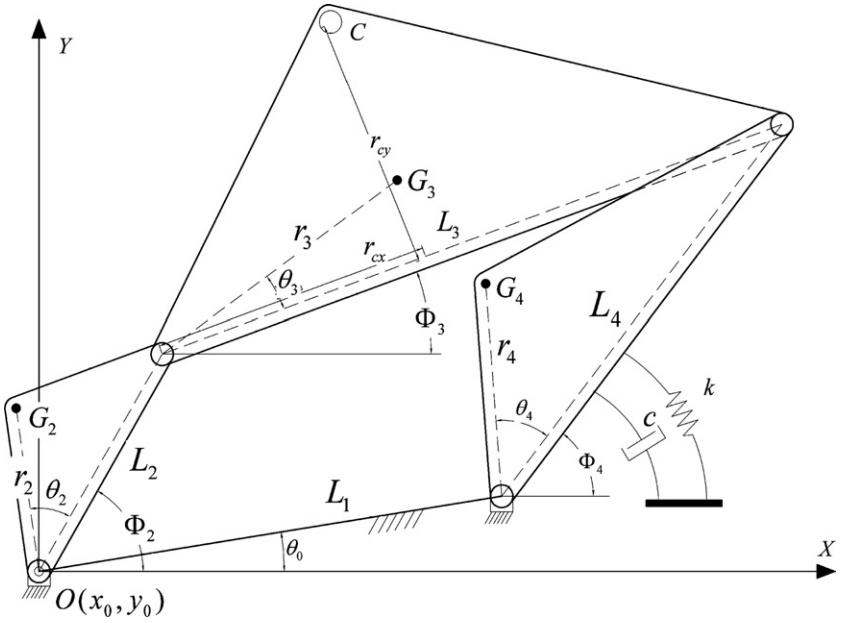

Fig. 1. Four-bar mechanism.

to reduce the motor power and to simplify the control strategy by reducing the driving torque variation as well as its fluctuation. Indeed, each change of the inertia, mass distribution of a mechatronic system yields a torque fluctuation and a velocity fluctuation of the motor.

4.1. The mechanism dynamic model

Fig. 1 shows a general four-bar mechanism. For link i ($i = 2, 3, 4$), the location of the center of mass is described by r_i and θ_i. m_i, L_i and J_i denote, respectively, the mass, the length and the inertia of link i. Using the angle Φ_2 as a generalized coordinate to describe the motion of the mechanism, one can write the equation of motion as

$$T = \frac{\mathrm{d}}{\mathrm{d}t}\left(\frac{\partial K}{\partial \dot{\Phi}_2}\right) - \frac{\partial K}{\partial \Phi_2} + \frac{\partial P}{\partial \Phi_2} + \frac{\partial D}{\partial \dot{\Phi}_2} \tag{12}$$

where T, K, P and D denote, respectively, the driving torque applied on the crank, the kinetic energy, the potential energy and the dissipative energy.

Replacing *all these quantities* by their expressions as a function of the mechanism parameters (see Appendix A), yields the following expression for the required torque to drive the mechanism:

$$T = A\ddot{\Phi}_2 + \frac{1}{2}\frac{\mathrm{d}A}{\mathrm{d}\Phi_2}\dot{\Phi}_2^2 + k_p(\Phi_2) + c\gamma_4^2\dot{\Phi}_2 \tag{13}$$

where the expressions of A, k_p, c, and γ_4 are given in Appendix A.

4.2. The driving motor model

In this section, we present the general dynamic model of a DC motor–gear system [5,9]. In Fig. 2, the input system is the voltage V, and the output of the system is the torque T_b, which is equal to the torque T defined in Eq. (13). R, L, e and i are, respectively, the armature resistance, the inductance, the electromotive force, and the current. J is the combined moment of inertia of the motor and the gear system. B is a damping coefficient due to possible viscous bearing friction. T_L is a constant mechanical load due, for instance, to brush friction, gear friction or dry bearing friction. The ratio of the geared speed-reducer is

$$n = \frac{T_b}{T_a} = \frac{\omega_a}{\omega_b} \tag{14}$$

Using the Kirchhoff's voltage law yields

$$V = Ri(t) + L\frac{\mathrm{d}i(t)}{\mathrm{d}t} + e \tag{15}$$

The equation of motion of the driving system is

$$T = n\left(T_{\mathrm{m}} - T_L - B\omega_a - J\frac{\mathrm{d}\omega_a}{\mathrm{d}t}\right) \tag{16}$$

where T_{m} is the magnetic motor torque. For a constant field current, this torque is

$$T_{\mathrm{m}} = K_{\mathrm{m}}i(t) \tag{17}$$

The constant electromotive force is

$$e = K_g\omega_a \tag{18}$$

where K_{m} and K_g are, respectively, the motor torque constant and the motor voltage constant.

Substituting Eqs. (14), (17) and (18) in Eqs. (15) and (16), we obtain

$$\frac{\mathrm{d}i(t)}{\mathrm{d}t} = \frac{1}{L}(V - Ri(t) + nK_g\dot{\Phi}_2) \tag{19}$$

And

$$T = nK_{\mathrm{m}}i(t) - nT_L - n^2B\dot{\Phi}_2 - n^2J\ddot{\Phi}_2 \tag{20}$$

Eqs. (19) and (20) represent the mathematical model of the DC motor. They give the current and motor torque variation with respect to time.

4.3. The mechatronic system model

For a mechatronic system, the torque produced by the motor (Eq. (20)) should be equal to the torque needed for the mechanical system (Eq. (13)). This equality is given by

$$nK_{\mathrm{m}}i(t) - nT_L - n^2B\dot{\Phi}_2 - n^2J\ddot{\Phi}_2 = A\ddot{\Phi}_2 + \frac{1}{2}\frac{\mathrm{d}A}{\mathrm{d}\Phi_2}\dot{\Phi}_2^2 + k_p(\Phi_2) + c\gamma_4^2\dot{\Phi}_2 \tag{21}$$

In order to simplify the control strategy and minimize the power of the motor, the velocity of the crank should be constant. With this assumption the second-order

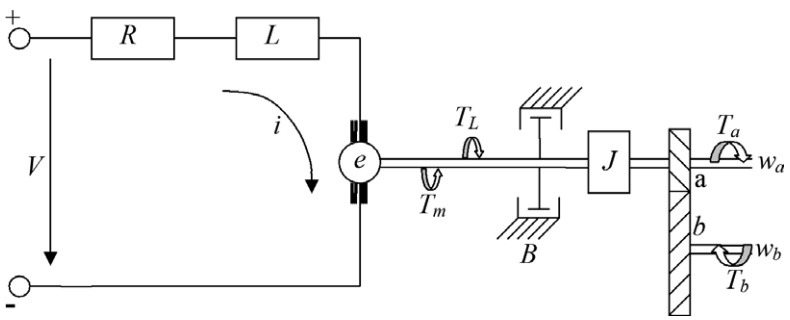

Fig. 2. Schematic of a DC motor-gear system.

derivative of Φ_2 in Eq. (21) will disappear and all the derivative of Φ_2 in Eqs. (19) and (21) are constant. Therefore, solving for $i(t)$, Eq. (21) becomes

$$i(t) = \frac{1}{nK_m}\left(\frac{1}{2}\frac{dA}{d\Phi_2}\dot{\Phi}_2^2 + k_p(\Phi_2) + c\gamma_4^2\dot{\Phi}_2 + nT_L + n^2B\dot{\Phi}_2\right) \quad (22)$$

where k_p is related to the torsional stiffness and the orientation of element 4 of the mechanism.

This equation gives the current required to maintain a constant crank speed at a steady state. It presents also, the second objective function that should be minimized.

The third objective function is the current variation:

$$\Delta i = \min(i_{max} - i_{min}) \quad (23)$$

where i_{min} and i_{max} are the lower and the upper current values during a cycle of motion of the mechanism.

Another objective function to minimize is the current fluctuation during a cycle.

From Eq. (22) we can write

$$\frac{di(t)}{dt} = \frac{1}{nK_m}\left\{\frac{1}{2}\dot{\Phi}_2^2\frac{d}{dt}\left(\frac{dA}{d\Phi_2}\right) + k\dot{\gamma}_4(\Phi_4 - \Phi_{4,0}) + k\gamma_4\dot{\Phi}_4 + 2c\gamma_4\dot{\gamma}_4\dot{\Phi}_2\right\} \quad (24)$$

See Appendixes A and B for details.

In what follows, we will assume that the external forces on the mechanism are zero, i.e., $k = 0$ and $c = 0$. Therefore, the objective function is then given by

$$\left|\frac{di(t)}{dt}\right|_{max} = \left|\frac{1}{2nK_m}\dot{\Phi}_2^2\frac{d}{dt}\left(\frac{dA}{d\Phi_2}\right)\right|_{max} \quad (25)$$

5. Results and discussions

In what follows, first, we will consider the problem of the dimensional synthesis to generate a given path. The obtained mechanism is then optimized to obtain the best mass distribution to minimize one of the following objective functions:

- The maximum current during a cycle (case 2).
- The maximum current variation (case 3).
- The maximum current fluctuation (case 4).

Finally, the global optimization approach is adopted (case 5). This approach is a multi-objective function optimization where several objective functions are considered simultaneously.

5.1. The optimization method

Genetic algorithms have been shown to solve linear and non-linear problems by exploring all regions of state space and exponentially exploiting promising areas through selection, crossover and mutation applied to individuals in population [14].

In the case of multi-objective GA (MOGA) optimization, the flowchart is illustrated in Fig. 3, where the outer loop represents one "evolutionary period" and the inner loop represents one GA "generation". In single objective GA, the inner loop (dashed line in Fig. 3) and the dashed boxes are omitted. The first step in the proposed MOGA is the generation of the individuals for the initial populations. Two populations have to be created randomly: static X_{st} and dynamic X_0. The static population is used to speed up the process by having a source of fresh individuals to be randomly added to the dynamic population at the beginning of each evolutionary period. This operation aims to maintain adequate population diversity.

For each individual of the dynamic population, the objective functions are evaluated. By using selection, crossover and mutation, it is possible to obtain a new population, X_{i+1}, from the current one, X_i, where "i" denotes the generation index. G_{max} is the maximum number of generations.

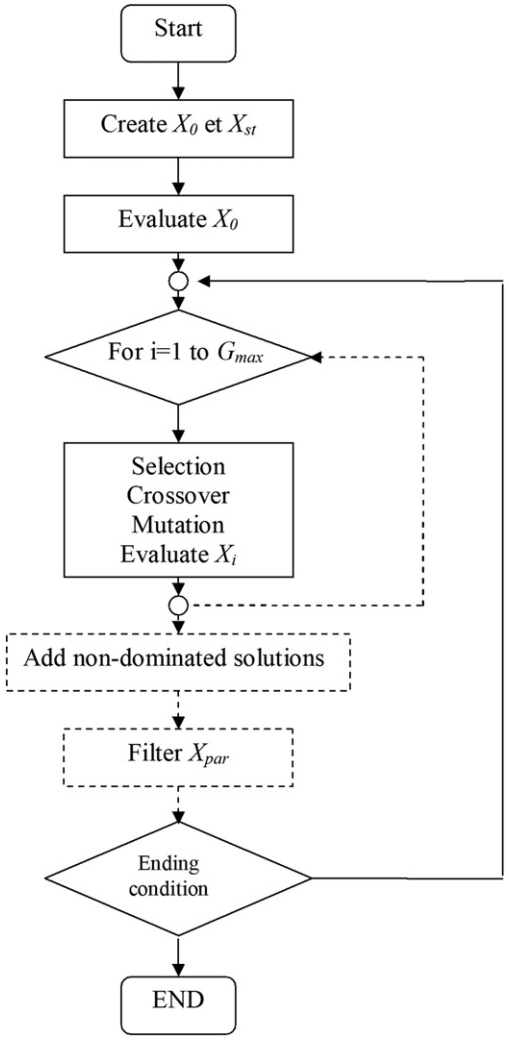

Fig. 3. The block diagram of the genetic algorithm.

In the selection operation, the following rules are used to compare a couple of individuals:

- A feasible individual (verifying all the constraints) is always better than an unfeasible one.
- In a couple of feasible individuals, one of them is better if it dominates the other one (yields lower values for all the objective functions). If not, both are equally good.
- A couple of unfeasible solutions are ranked according to the "amount of unfeasibility", i.e., how far is the violation of the constraint and how many constraints are violated.

At the end of each evolutionary period, the non-dominated individuals (Paretian solutions) are selected from the dynamic population and added to the elitist one (Paretian population). This elitist population is then filtered to yield a non-dominated population. To begin a new evolutionary period, the new dynamic population is randomly generated from the static population and the current dynamic population. The evolutionary process is stopped after a maximum number of "evolutionary periods".

For the multi-objective optimization, the optimum solutions form what is called a "Pareto Front". These solutions correspond to the non-dominated individuals which present the best solution for all the objective functions simultaneously. Otherwise the individuals are called dominated.

Therefore, the algorithm scans the whole search domain and compares all the individuals to keep only those that are not dominated. The designer can then choose, among all possible solutions, the one that suites best his application. For three objective functions, the "Pareto front" is a surface in a three-dimensional space. For n objective functions the Pareto front is a hyperplane in an n-dimensional space. More details about this method could be found in [13].

The parameters of the optimization algorithm are: the crossover probability PC = 0.9 and the mutation probability PM = 0.1, the maximum number of generations, G_{max}, is different for each case.

5.2. Dimensional synthesis of the mechanism (case 1)

The presented results are given by the GA mono-objective optimization. A total of 16 points ($N = 16$) on the desired curve are specified. The bounding intervals for each one of the variables are given between zero and 500 mm. The ending condition depends only on the number of generations. The total error is significantly reduced at 96% after 100 iterations (in Fig. 4a). With these parameters of GA, the final error of the optimized mechanical system is $e = 4.43$ mm, where e is given by

$$e = \left(\sum_{i=1}^{N} [(C_{xd}^i - C_{xr}^i)^2 + (C_{yd}^i - C_{yr}^i)^2] \right)^{\frac{1}{2}} \quad (26)$$

The desired curve is shown in Fig. 4b along with the curve generated by the optimum mechanism.

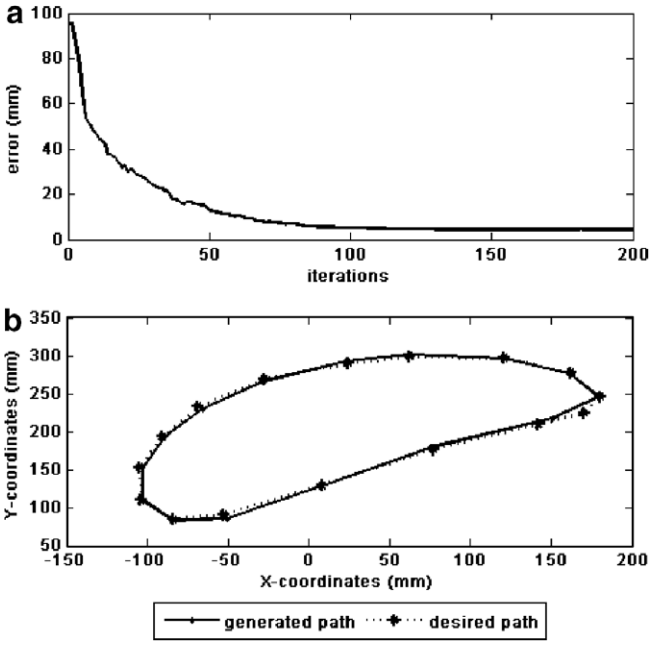

Fig. 4. Result of the dimensional synthesis of the mechanism. (a) Rate of convergence of the objective function, (b) the desired path along with the generated one.

Table 1
Dimensions of the optimal mechanism (m)

L_1	L_2	L_3	L_4	r_{cx}	r_{cy}
0.246	0.111	0.295	0.186	0.145	0.152

Table 1, contains the optimized link lengths of the mechanism. The obtained dimensions of the mechanism will be taken as input parameters to find the optimal mass distribution in order to reduce the maximum current, the current variation and the current fluctuation in the driving motor.

5.3. Optimization of the mechatronic system

The characteristics of the motor used in this work are given in Table 2.

5.3.1. Case 1: non-optimized system

In this section, we will assume that the mass of each link is uniformly distributed. Therefore, the location of the center of mass and the moment of inertia of each link are given, respectively, by $L/2$ and $mL^2/12$, where m its mass and L its length (Table 3). The crank is assumed balanced; hence its center of mass is located in the center of its joint with the ground.

Fig. 5c presents the mechanism with a non-optimized mass distribution (case 1) with the graph of the current during two cycles of motion (Fig. 5a). We can notice that for a non-optimized mechatronic system (only the geometry is optimized) the current drained by the motor is highly variable, with a maximum current $i_{max} = 5.42$ A,

Table 2
Motor parameters

R (Ω)	L (H)	K_m (N m/a)	K_g (V s)	J (kg m^2)	T_L (N m)	B (N ms)
0.4	0.05	0.678	0.678	0.056	0.0	0.226

Table 3
The optimized design vector of the non-optimized mechatronic system

r_3 (m)	r_4 (m)	θ_3 (°)	θ_4 (°)	m_3 (kg)	m_4 (kg)	j_3 (kg m^2)	j_4 (kg m^2)
0.148	0.093	0	0	5.54	3.6	0.0133	0.0086

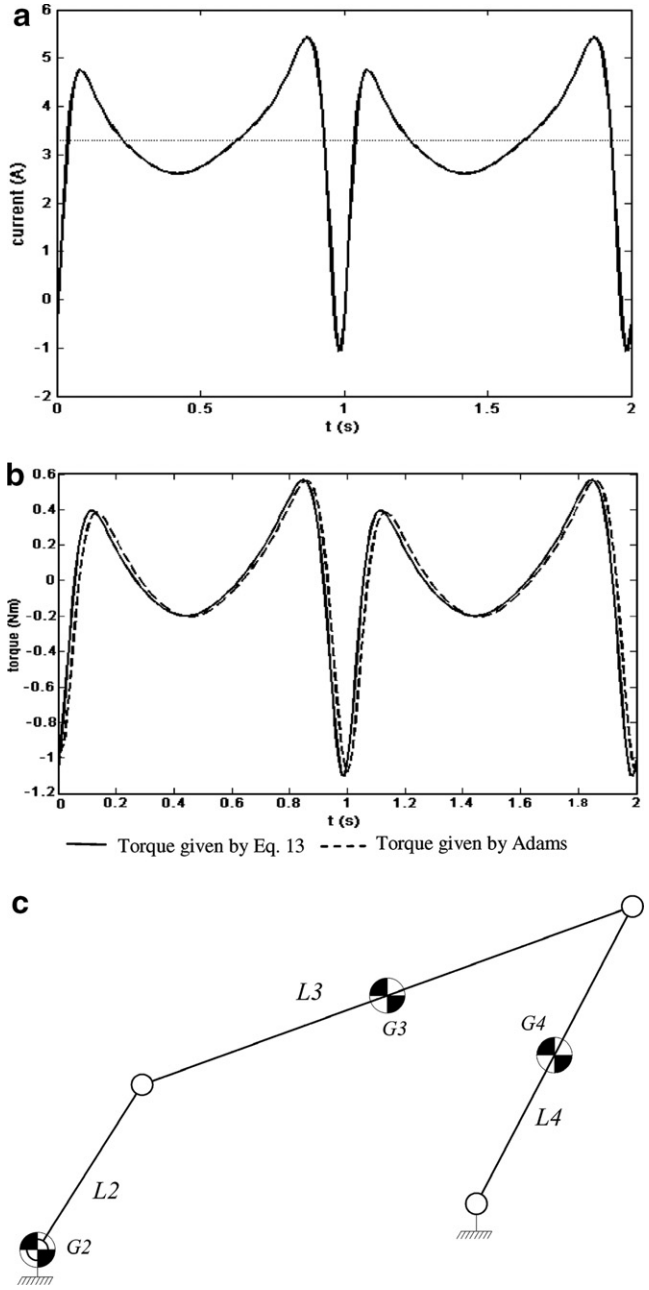

Fig. 5. The non-optimized mechatronic system. (a) Variation of the current, (b) validation of the analytic dynamic model and (c) mechanism with a non-optimized mass distribution.

a current variation $\Delta i = 6.48$ A and the current fluctuation $\left|\frac{di(t)}{dt}\right|_{max} = 67.9$ A/s.

The commercial software ADAMS was used to validate our dynamic model (Eq. (13)). Fig. 5b presents the graph of the torque given by ADAMS and the one given by Eq. (13). We can notice that the two results are in good agreement. Since the current drained by the motor is proportional to the torque and in order to optimize the totality of the mechatronic system, we will express in what follows all our objective functions in terms of the current and its variation.

5.3.2. Case 2: minimization of the maximum current

The goal in what follows is to optimize the mass distribution, for the given dimensions, of the mechanism that minimize the maximum current of the mechatronic system. This goal can be expressed by the objective function derived from Eq. (22). It is expressed as follows (case 2):

$$f_2 : \min(i(t)_{max}) \tag{27}$$

Subject to:

$$\begin{cases} g_1 : \dot{\Phi}_2 = \text{constant} \\ g_2(X) : x_i \in [x_{i\min}, x_{i\min}], \quad x_i \in X \end{cases} \tag{28}$$

The design vector to be optimized is

$$X = [r_3, r_4, \theta_3, \theta_4, m_3, m_4, j_3, j_4] \tag{29}$$

In this example, the maximum number of generations is $G_{max} = 100$.

Fig. 6a shows the value of the objective function during the optimization process. One can notice that the final value of the objective function is attained after only 10 generations.

We can notice that the GA method reduced the maximum current by a factor of 2.5 compared to the one given in case 1. However, the current variation is still high ($\Delta i = 2.14$ A) even though it was reduced by a factor of 3 compared to case 1 ($\Delta i = 6.48$ A). The current fluctuation is, however, still high $\left|\frac{di(t)}{dt}\right|_{max} = 38.47$ A/s.

The current variation during two cycles is given in Fig. 6a, whereas the optimized mechanism is given in Fig. 6b. The design vector is given in Table 4.

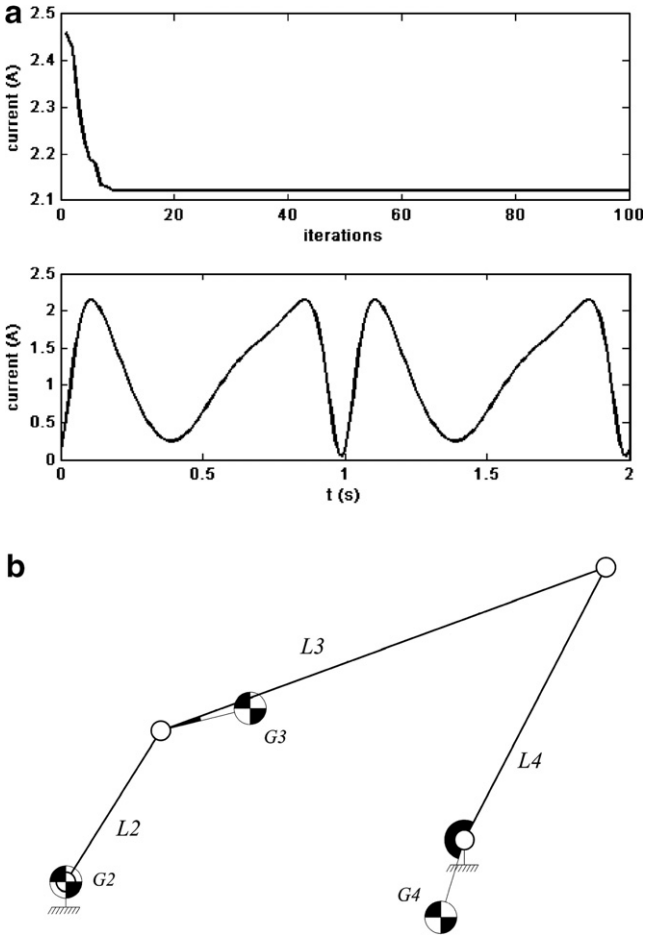

Fig. 6. Optimization results for minimizing i_{max}. (a) Algorithm convergence and (b) optimized mechanism that minimizes the maximum current.

5.3.3. Case 3: minimization of the current variation

In order to simplify the control strategy, the designer of a mechatronic system should minimize the current variation. In general, for a simple PID controller, the gains are constant therefore the current should have as little variation as possible to have an acceptable behavior of the controlled system.

The objective function to be minimized over a cycle of motion is the maximum variation. In this case (case 3):

$$f_3 : \min(\Delta i) \tag{30}$$

where

$$\Delta i = i_{max} - i_{min} \tag{31}$$

The constraints and the design vector are the same as in case 2. The maximum number of generations is also the same as in case 2.

Fig. 7a shows the value of the objective function during the optimization process. One can notice that the final value of the objective function is obtained after only 20 generations. The maximum current variation is $\Delta i = 1.63$ A (Fig. 7a). Therefore, a reduction by a factor of 4 with respect to the non-optimized mechanism is obtained and 20% with respect to the mechanism where the maximum current was minimized. However, the current fluctuation is still high $\left|\frac{di(t)}{dt}\right|_{max} = 33.6$ A/s, even though it was reduced by a factor of 2 with respect to case 1.

The obtained mechanism is given by Fig. 7b. The optimized design vector is given in Table 5.

5.3.4. Case 4: minimization of the current fluctuation

Minimizing the maximum current or its maximum variation does not guarantee that the obtained current is

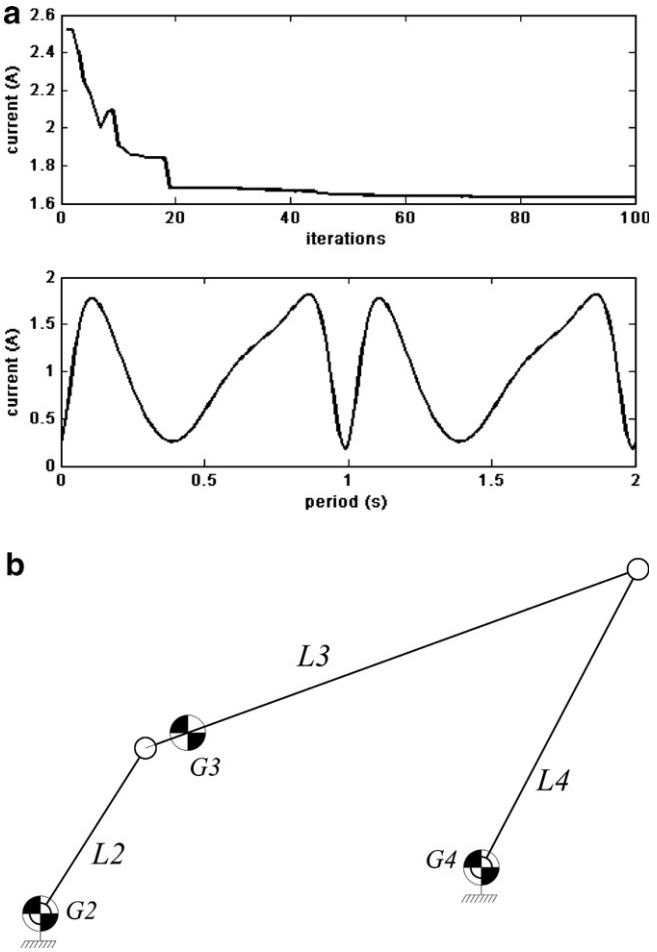

Fig. 7. Optimization of the current variation. (a) Algorithm convergence and (b) optimized mechanism that minimizes the current variation.

Table 4
Optimized design vector that minimizes the maximum current

r_3 (m)	r_4 (m)	θ_3 (°)	θ_4 (°)	M_3 (kg)	m_4 (kg)	j_3 (kg m^2)	j_4 (kg m^2)
0.057	0.050	353.7	191.4	2.49	1.20	0.0133	0.0086

Table 5
Optimized design vector that minimizes the current variation

r_3 (m)	r_4 (m)	θ_3 (°)	θ_4 (°)	m_3 (kg)	m_4 (kg)	j_3 (kg m^2)	j_4 (kg m^2)
0.0253	0	360	0	4.47	3.59	0.0133	0.0086

optimal for the driving motor. Indeed, if the current fluctuation $\left(\left|\frac{\mathrm{d}i(t)}{\mathrm{d}t}\right|_{\max}\right)$ is too high it would mean high voltage, which present undesirable solicitation, in the motor (Eq. (15)). Therefore, finding the best mass distribution capable of reducing the current fluctuation is necessary to avoid the motor being highly loaded. The objective function, in this case, is given by

$$f_4 : \min\left(\left|\frac{\mathrm{d}i(t)}{\mathrm{d}t}\right|_{\max}\right) \tag{32}$$

The maximum number of generations is $G_{\max} = 50$. The obtained results are given in Fig. 8 and Table 6. The current fluctuation is $\left|\frac{\mathrm{d}i(t)}{\mathrm{d}t}\right|_{\max} = 25$ A/s.

A reduction of $\left|\frac{\mathrm{d}i(t)}{\mathrm{d}t}\right|_{\max}$ by 25% is obtained compared to the previous case for about the same current variation ($\Delta i = i_{\max} - i_{\min} = 1.75$ A). Therefore, one can conclude that the $\left|\frac{\mathrm{d}i(t)}{\mathrm{d}t}\right|_{\max}$ criterion can be a better one than $\Delta i = i_{\max} - i_{\min}$, since it can yield better results on both quantities. We will retain, then, only $\left|\frac{\mathrm{d}i(t)}{\mathrm{d}t}\right|_{\max}$ as criterion to be minimized for the global optimization.

5.3.5. Case 5: global synthesis of the mechatronic system

If we compare the mass distribution obtained in case 2, case 3, and case 4, we can notice that the obtained mass distribution for the different links of the mechanism are different. However, it would be more interesting if we can find a mechanism that minimizes all the previous objective functions simultaneously. This objective can be reached by using the multi-objective optimization. The following objective functions are selected to be minimized simultaneously (case 5):

$$f_1 : \min\left(\sum_{i=1}^{N}\left[(C^i_{xd} - C^i_x)^2 + (C^i_{yd} - C^i_y)^2\right]. \right.$$
$$\left. + M_1 h_1(X) + M_2 h_2(X) + M_3 h_3(X)\right) \tag{33}$$

$$f_2 : \min(i(t)_{\max}) \tag{34}$$

$$f_4 : \min\left(\left|\frac{\mathrm{d}i(t)}{\mathrm{d}t}\right|_{\max}\right) \tag{35}$$

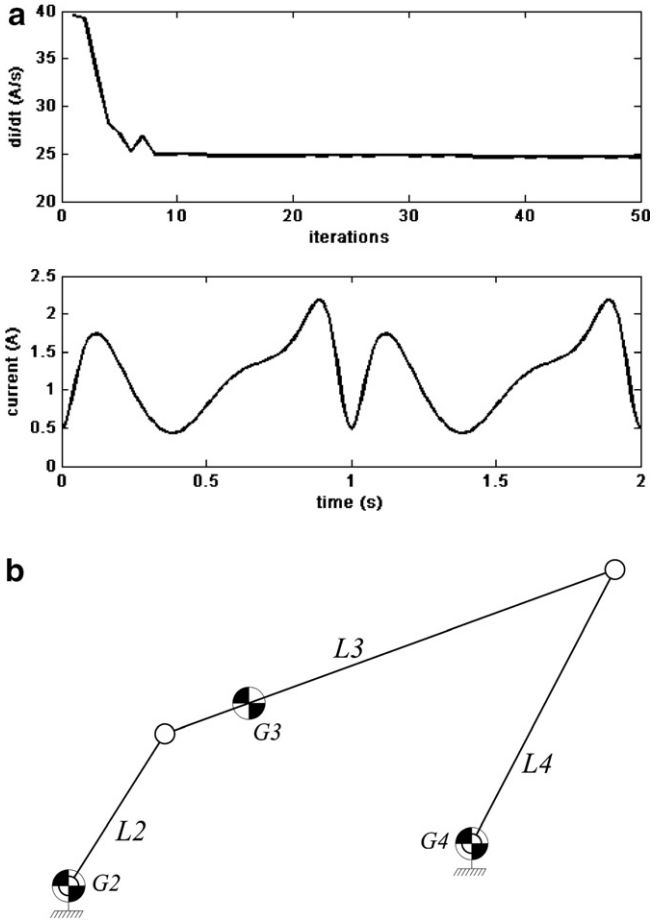

Fig. 8. Optimization results for the current fluctuation. (a) Algorithm convergence and (b) optimized mechanism that minimizes the current fluctuation.

Subject to:

$$\begin{aligned} &g_1 : \dot{\Phi}_2 = \text{constant} \\ &g_2 : x_i \in [x_{i\min}, x_{i\min}], \quad x_i \in X \\ &g_3(X) : \Phi_{2,i} - \Phi_{2,i+1} < 0 \\ &g_4(X) : L_1 + L_2 < L_3 + L_4; \quad L_2 < L_3 < L_4 < L_1 \end{aligned} \tag{36}$$

The design vector to be optimized is

$$X = [L_i, \Phi_{2k}, r_{cx}, r_{cy}, r_3, r_4, \theta_3, \theta_4, m_3, m_4, j_3, j_4] \quad (k = 1, \ldots, 16) \tag{37}$$

Table 6
Optimized design vector that minimizes the current fluctuation

r_3 (m)	r_4 (m)	θ_3 (°)	θ_4 (°)	m_3 (kg)	m_4 (kg)	j_3 (kg m^2)	j_4 (kg m^2)
0.034	0	343.9	215.3	2.17	1.20	0.0133	0.0086

The optimization method used here, is based on the Pareto dominance principle. The initial populations X_{st} and X_0 is made of 2000 individuals, the paretian population, X_{par}, is made of 1942 non-dominated individuals. Fig. 9 shows the surface representing the Pareto front (Non-dominated population). Each point represents the values of the three objective functions obtained by a given design vector. One can also notice that the current and its fluctuation, for a given path error, vary in the opposite directions. Four selected points are shown in Fig. 9 and the corresponding design vectors are shown in Table 7.

In the previous cases (case 1, case 2 and case 4), see Table 8, the geometric parameters of the mechanism were fixed and the minimum value of $\left|\frac{di(t)}{dt}\right|_{max}$ that could be obtained was around 25 A/s. However, solution number 4 in Table 7 allowed us to have $\left|\frac{di(t)}{dt}\right|_{max} = 15.76$ A/s, whereas the error on the obtained path increased from $e = 4.43$ (case 2, case 3 and case 4) to $e = 21.84$ mm (case 5, Solution No. 4). Therefore, the multi-objective optimization can explore other domains for possible solutions that the sequential approach cannot reach.

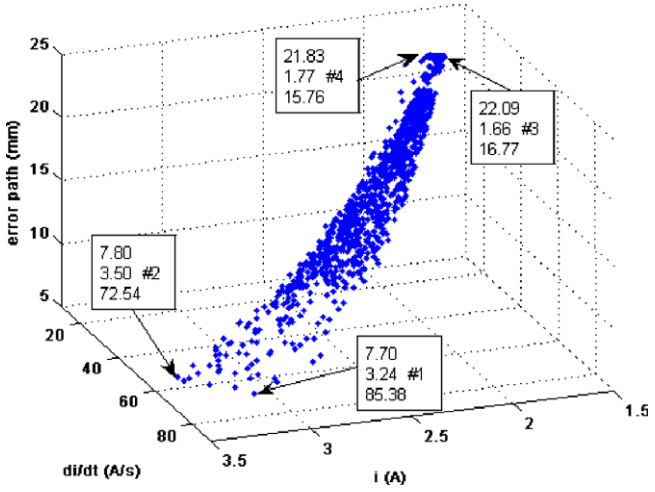

Fig. 9. Global optimization of the mechatronic system.

Table 7
Design vectors of the four selected points

Design vector	# 1	# 2	# 3	# 4
r_3 (m)	0.0195	0.0206	0.0198	0.0200
r_4 (m)	0.0040	0.0050	0	0
θ_3 (°)	344.82	343.97	343.94	344.78
θ_4 (°)	0	110.39	360.18	360.18
m_3 (kg)	5.35	3.65	4.26	2.95
m_4 (kg)	3.60	3.60	3.60	3.53
j_3 (kg m^{-2})	0.0133	0.0133	0.0133	0.0133
j_4 (kg m^{-2})	0.0086	0.0086	0.0086	0.0086
L_1 (m)	0.250	0.249	0.250	0.250
L_2 (m)	0.108	0.107	0.80	0.80
L_3 (m)	0.290	0.290	0.290	0.290
L_4 (m)	0.190	0.190	0.190	0.190
r_{cx} (m)	0.145	0.145	0.155	0.155
r_{cy} (m)	0.150	0.150	0.153	0.155

Table 8
Design vectors of the different cases

Design vector	Case 1	Case 2	Case 4	Case 5
L_1 (m)	0.246	0.246	0.246	0.250
L_2 (m)	0.111	0.111	0.111	0.080
L_3 (m)	0.295	0.295	0.295	0.290
L_4 (m)	0.186	0.186	0.186	0.190
r_{cx} (m)	0.145	0.145	0.145	0.155
r_{cy} (m)	0.152	0.152	0.152	0.155
r_3 (m)	0.150	0.057	0.034	0.0200
r_4 (m)	0.099	0.05	0	0
θ_3 (°)	0	353.7	343.9	344.82
θ_4 (°)	0	191.4	215.3	360.18
m_3 (kg)	5.54	2.49	2.17	2.95
m_4 (kg)	3.60	1.20	1.20	3.53
j_3 (kg m^{-2})	0.0133	0.0133	0.0133	0.0133
j_4 (kg m^{-2})	0.0086	0.0086	0.0086	0.0086
Objective functions				
Path error (mm)	4.43	4.43	4.43	21.84
Current (A)	5.42	2.14	2.20	1.77
Current fluctuation $\lvert di/dt\rvert$ (A/s)	67.90	38.47	25.00	15.76

From the presented four possible solutions (Fig. 9), one can notice that the third solution presents the advantage of having the minimum current and the first one has the minimum path error and finally the fourth one has the minimum current fluctuation. Between the third solution and the fourth one, we have an increase of about 7% in the current and a reduction of about 6.5% in the current fluctuation (Fig. 10).

For case 5, the generated path presented in Fig. 12 and the current fluctuation, presented in Fig. 11, correspond to solution No. 4. We can notice that the generated paths of the sequential and multi-objective optimization are fairly close. Therefore, we state that the solution given in case 5 is the most interesting one in terms of current and current fluctuation despite an increase in the path error. However, the designer can use any other optimized design vector,

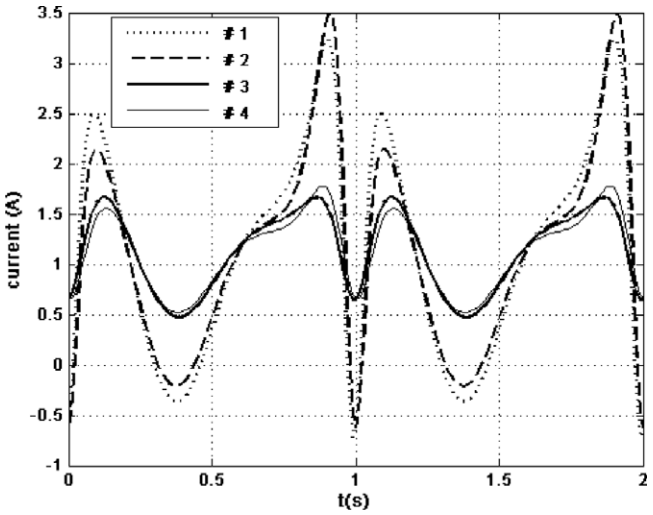

Fig. 10. Current fluctuation of the four selected point.

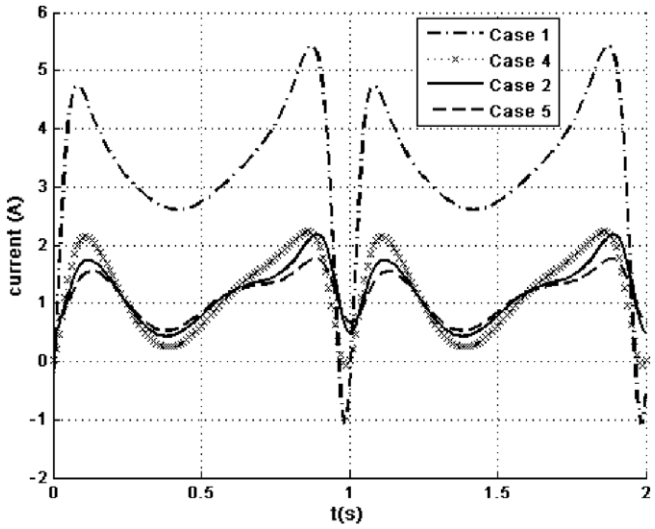

Fig. 11. Current fluctuation of the different cases.

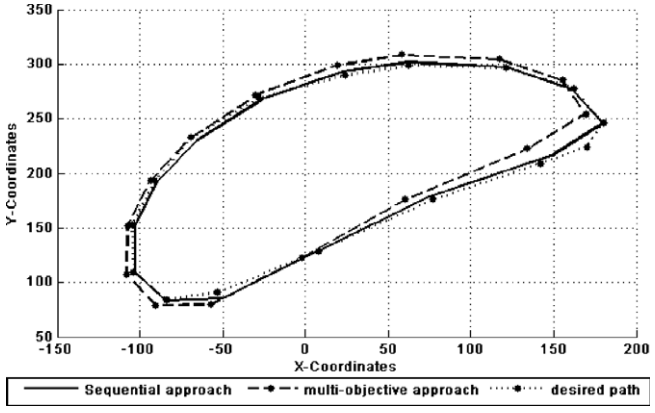

Fig. 12. Path errors of the sequential and multi-objective optimizations.

corresponding to any of the solutions presented by the Pareto front, which suits best his application.

6. Conclusion

This work dealt with the problem of optimizing the geometry and the dynamic behavior of a four-bar mechatronic system. First, we presented the sequential approach where we optimized sequentially the geometry of the mechanism, for a given path, and then solved the dynamic problem where we take into account the characteristics of the motor along with the inertia of the different links of the mechanism. Several types of objective functions were tested: the maximum current used by the motor, its maximum variation, and finally its fluctuation. We showed that, when we use the geometric parameters given by the path synthesis problem to try to optimize the dynamic behavior of the mechatronic system, we could not obtain optimal results. A global optimization problem was then formulated where all the parameters of the mechanism were considered simultaneously, and the problem is presented as a multi-objective optimization one where the geometry and the dynamics were considered simultaneously. The obtained solutions form what is called a "Pareto front". These solutions are then analyzed for several different design conditions. We show, for example, that a small increase in the error of the generated path, allowed us to a significant decrease the current fluctuation. This paper also shows the advantages of a multi-objective optimization approach over the mono-objective one.

Acknowledgment

This work was partially supported by the "Ministère de la recherche scientifique et de la technologie et du développement des compétences" under the Contract SERST LAB-MA-05.

Appendix A

The kinetic energy is expressed as follows:

$$K = \sum_{i=2}^{4} \left(\frac{1}{2} m_i V_i^2 + \frac{1}{2} J_i \dot{\Phi}_i^2 \right), \quad i = (2,3,4) \tag{A.1}$$

where V_i is the velocity of the center of masse G_i given by

$$\vec{V}_i = \vec{\alpha}_i \dot{\Phi}_2 \quad (i = 2,3,4) \tag{A.2}$$

where

$$\vec{\alpha}_2 = [-r_2 \sin(\Phi_2 + \theta_2)\vec{x} + r_2 \cos(\Phi_2 + \theta_2)\vec{y}] \tag{A.3}$$

$$\vec{\alpha}_3 = [(-L_2 \sin \Phi_2 - r_3 \gamma_3 \sin(\Phi_3 + \theta_3))\vec{x} + (L_2 \cos \Phi_2 + r_3 \gamma_3 \cos(\Phi_3 + \theta_3))\vec{y}] \tag{A.4}$$

$$\vec{\alpha}_4 = [-r_4 \gamma_4 \sin(\Phi_4 + \theta_4)\vec{x} + r_4 \gamma_4 \cos(\Phi_4 + \theta_4)\vec{y}] \tag{A.5}$$

where γ_3 and γ_4 are defined in what is follows:

$$\gamma_3 = -\frac{L_2 \sin(\Phi_2 - \Phi_4)}{L_3 \sin(\Phi_3 - \Phi_4)} \tag{A.6}$$

$$\gamma_4 = \frac{L_2 \sin(\Phi_2 - \Phi_3)}{L_4 \sin(\Phi_4 - \Phi_3)} \tag{A.7}$$

The derivative of the dissipative energy is given by

$$\frac{\partial D}{\partial \dot{\Phi}_2} = \frac{1}{2} c \gamma_4^2 \dot{\Phi}_2^2 \tag{A.8}$$

The potential energy is expressed as follows:

$$P = \frac{1}{2} k (\Phi_4 - \Phi_{4,0})^2 \tag{A.9}$$

$$k_p(\Phi_2) = \frac{\partial P}{\partial \Phi_2} = k \gamma_4 (\Phi_4 - \Phi_{4,0}) \tag{A.10}$$

$\Phi_{4,0}$ is the angle where the spring is unloaded.

The expression of $A(\Phi_2)$ and $\frac{dA(\Phi_2)}{d\Phi_2}$ are given, respectively, by

$$A(\Phi_2) = J_2 + m_2 r_2^2 + m_3 L_2^2 + (J_3 + m_3 r_3^2)\gamma_3^2 + (J_4 + m_4 r_4^2)\gamma_4^2 + 3m_3 r_3 L_2 \gamma_3 \cos(\Phi_3 - \Phi_2 + \theta_3) \tag{A.11}$$

$$\frac{dA}{d\Phi_2} = 2(J_3 + m_3 r_3^2)\gamma_3 \frac{L_2(D_1 + D_2)}{L_3 \sin^2(\Phi_3 - \Phi_4)} + 2(J_4 + m_4 r_4^2)\gamma_4 \frac{L_2(D_3 + D_4)}{L_4 \sin^2(\Phi_3 - \Phi_4)} + 3m_3 r_3 L_2 \left\{ \frac{d\gamma_3}{d\Phi_2} \cos(\Phi_3 - \Phi_2 + \theta_3) - \gamma_3 \sin(\Phi_3 - \Phi_2 + \theta_3)(\gamma_3 - 1) \right\} \tag{A.12}$$

where

$$\begin{aligned} D_1 &= (\gamma_4 - 1)\sin(\Phi_3 - \Phi_4)\cos(\Phi_4 - \Phi_2) \\ D_2 &= \sin(\Phi_4 - \Phi_2)\cos(\Phi_3 - \Phi_4)(\gamma_4 - \gamma_3) \\ D_3 &= (\gamma_3 - 1)\sin(\Phi_3 - \Phi_4)\cos(\Phi_3 - \Phi_2) \\ D_4 &= \sin(\Phi_3 - \Phi_2)\cos(\Phi_3 - \Phi_4)(\gamma_4 - \gamma_3) \end{aligned} \tag{A.13}$$

Appendix B

$$\frac{di(t)}{dt} = \frac{1}{nK_m}\left\{ \frac{1}{2}\dot{\Phi}_2^2 \frac{d}{dt}\left(\frac{dA}{d\Phi_2}\right) + k\dot{\gamma}_4(\Phi_4 - \Phi_{4,0}) + k\gamma_4\dot{\Phi}_4 + 2c\gamma_4\dot{\gamma}_4\dot{\Phi}_2 \right\} \tag{B.1}$$

If we take $k = 0$ and $c = 0$ (no external loading), we can write

$$\frac{di(t)}{dt} = \frac{1}{nK_m}\left\{ \frac{1}{2}\dot{\Phi}_2^2 \frac{d}{dt}\left(\frac{dA}{d\Phi_2}\right) \right\} \tag{B.2}$$

where

$$\frac{d}{dt}\left(\frac{dA}{d\Phi_2}\right) = \frac{d^2A}{d\Phi_2^2}\dot{\Phi}_2 = (F_1 + F_2 + F_3)\dot{\Phi}_2$$

The quantities F_1, F_2, F_3 are given by

$$F_1 = 2(J_3 + m_3 r_3^2)\left(\left(\frac{d\gamma_3}{d\Phi_2}\right)^2 + \gamma_3 \frac{d^2\gamma_3}{d\Phi_2^2} \right) \tag{B.3}$$

$$F_2 = 2(J_4 + m_4 r_4^2)\left(\left(\frac{d\gamma_4}{d\Phi_2}\right)^2 + \gamma_4 \frac{d^2\gamma_4}{d\Phi_2^2} \right) \tag{B.4}$$

$$F_3 = 3m_3 r_3 L_2 \left[\left(\frac{d^2\gamma_3}{d\Phi_2^2} - \gamma_3(\gamma_3 - 1)^2 \right)\cos(\Phi_3 - \Phi_2 + \theta_3) - (3\gamma_3 - 2)\frac{d\gamma_3}{d\Phi_2}\sin(\Phi_3 - \Phi_2 + \theta_3) \right] \tag{B.5}$$

References

[1] Wu FX, Zhang WJ, Li Q, Ouyang PS. Integrated design and PD control of high-speed closed-loop mechanisms. ASME J Dyn Syst Meas Control 2002;124:522–8.

[2] Ouyand PR, Li Q, Zhang WJ, Guo LS. Design, modeling and control of hybrid machine system. Mechatronics 2004;14:1197–217.

[3] Tang KZ, Huang SN, Tan KK, Lee TH. Combined PID and adaptive nonlinear control for servo mechanical systems. Mechatronics 2004;14:701–14.

[4] Li Q, Wu FX. Control performance improvement of parallel robot via the design for control approach. Mechatronics 2004;14:947–64.

[5] Klafter RD, Chmielewski TA, Negin M. Robotic engineering an integrated approach. Prentice-Hall, Inc.; 1989.

[6] Zhang WJ, Li Q, Guo LS. Integrated design of mechanical structure and control algorithm for programmable four-bar linkage. IEEE/ASME Trans Mech 1999;4(4):354–62.

[7] Gündogdu Ö, Erentürk K. Fuzzy control of a dc motor driven four-bar mechanism. Mechatronics 2005;15:423–38.

[8] Cabrera JA, Simon A, Prado M. Optimal synthesis of mechanisms with genetic algorithms. Mech Mach Theory 2002;37:1165–77.

[9] Tao J, Sadler JP. Constant speed control of a motor driven mechanism system. Mech Mach Theory 1995;30(5):737–48.

[10] Laribi MA, Mlika A, Romdhane L, Zeghloul S. A combined genetic algorithm–fuzzy logic method (GA–FL) in mechanisms synthesis. Mech Mach Theory 2004;39(7):665–795.

[11] Straete HJ, Schutter JD. Hybrid cam mechanisms. IEEE/ASME Trans Mech 1996;1(4):284–9.

[12] Zhang O, Xu Z, Mechefske CHM, Xi F. Optimum design of parallel kinematic tool heads with genetic algorithms. Robotica 2004;22:77–84.

[13] Sardinas RQ, Santana MR, Brindis EA. Genetic algorithm-based multi-objective optimization of cutting parameters in turning processes. Eng Appl Artif Intell 2006;16:127–33.

[14] Goldberg DE. Genetic algorithms in search, optimization and machine learning. Longman: Addison-Wesley; 1989.

[15] Bi ZM, Zhang WJ. Concurrent optimal design of modular robotic configuration. J Rob Syst 2001;18(2):77–87.